

Part123: Part-aware 3D Reconstruction from a Single-view Image

Anran Liu*
liuar616@connect.hku.hk
The University of Hong Kong
Hong Kong, China

Xiaoxiao Long†
xxlong@connect.hku.hk
The University of Hong Kong
Hong Kong, China

Cheng Lin*
chlin@connect.hku.hk
The University of Hong Kong
Hong Kong, China

Zhiyang Dou
zhiyang0@connect.hku.hk
The University of Hong Kong
Hong Kong, China

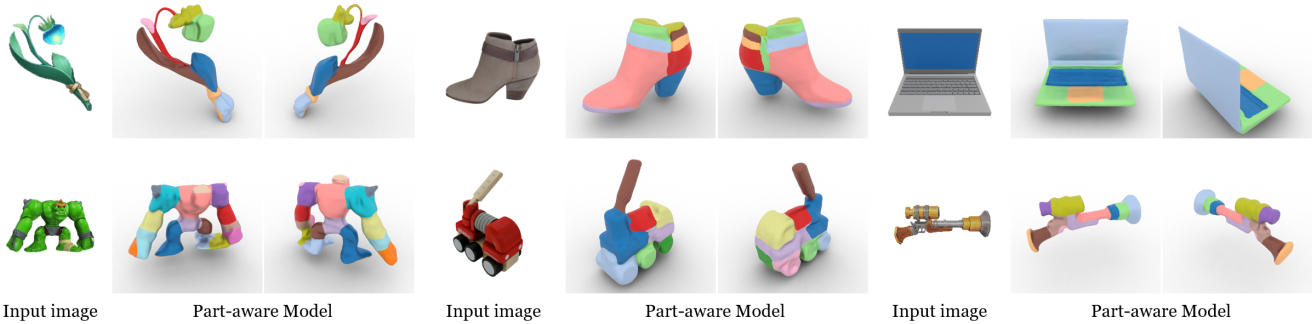
Yuan Liu
liuyuanwhuer@gmail.com
The University of Hong Kong
Hong Kong, China

Hao-Xiang Guo
guohaoxiangxiang@gmail.com
Tsinghua University
Beijing, China

Ping Luo
pluo@cs.hku.hk
The University of Hong Kong
Hong Kong, China

Wenping Wang†
wenping@tamu.edu
Texas A&M University
College Station, USA

Part-aware Reconstruction



Primitive-based Reconstruction

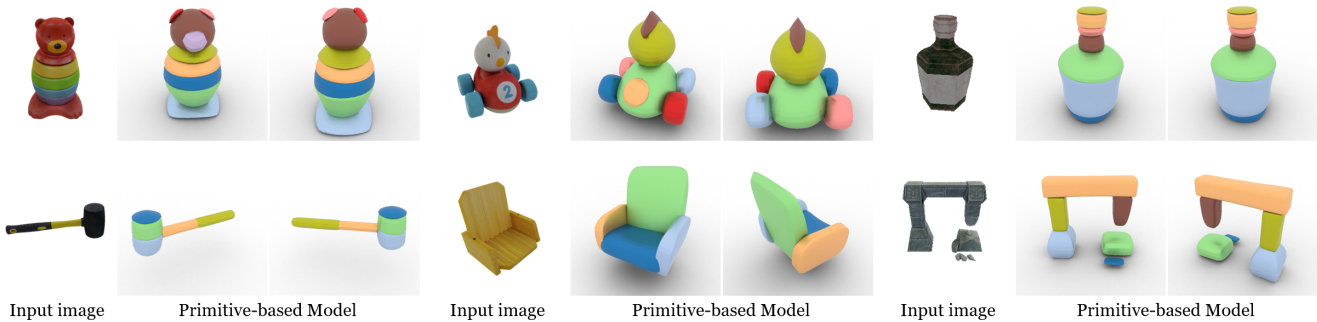


Figure 1: Part-aware 3D models generated from single-view images using Part123. Our method generates 3D models with structurally meaningful part segmentation for various objects (1st and 2nd rows). Our part-aware reconstruction can also benefit many shape-processing tasks, such as primitive-based reconstruction (3rd and 4th rows). Based on the information of part segments, the shape can be well fitted into multiple simple primitives, like the deformed superquadrics for high-level shape abstraction.

ABSTRACT

Recently, the emergence of diffusion models has opened up new opportunities for single-view reconstruction. However, all the existing

methods represent the target object as a closed mesh devoid of any structural information, thus neglecting the part-based structure, which is crucial for many downstream applications, of the reconstructed shape. Moreover, the generated meshes usually suffer from large noises, unsmooth surfaces, and blurry textures, making it challenging to obtain satisfactory part segments using 3D segmentation

*Both authors contributed equally to this research.

† Corresponding authors.

techniques. In this paper, we present **Part123**, a novel framework for part-aware 3D reconstruction from a single-view image. We first use diffusion models to generate multiview-consistent images from a given image, and then leverage Segment Anything Model (SAM), which demonstrates powerful generalization ability on arbitrary objects, to generate multiview segmentation masks. To effectively incorporate 2D part-based information into 3D reconstruction and handle inconsistency, we introduce contrastive learning into a neural rendering framework to learn a part-aware feature space based on the multiview segmentation masks. A clustering-based algorithm is also developed to automatically derive 3D part segmentation results from the reconstructed models. Experiments show that our method can generate 3D models with high-quality segmented parts on various objects. Compared to existing unstructured reconstruction methods, the part-aware 3D models from our method benefit some important applications, including feature-preserving reconstruction, primitive fitting, and 3D shape editing.

1 INTRODUCTION

Reconstructing an object from its single-view image is a demanding task in visual computing. Humans have been granted an impressive cognitive ability to reason about the 3D information from a single-view observation, yet it is still a challenging ill-posed problem for machines due to the lack of 3D hints in a single image. Recent advances in deep learning have opened up new opportunities in single-view reconstruction, especially diffusion models with powerful generation capacity [Ho et al. 2020; Liu et al. 2023a; Long et al. 2023a; Melas-Kyriazi et al. 2023; Qian et al. 2023; Sohl-Dickstein et al. 2015; Tang et al. 2023].

Despite the great progress, existing methods pay little attention to distinguishing different components of the reconstructed models. These methods generally build the 3D model as a whole without any structural information. The part-based structure of 3D models is crucial for many real-world applications [Rodrigues et al. 2018], including shape modelling [Funkhouser et al. 2004; Ji et al. 2006], shape retrieval [Ferreira et al. 2010; Zuckerberger et al. 2002], texture mapping [Lévy et al. 2002; Sander et al. 2003] and animation [Yuan et al. 2016]. Although many methods exist for direct segmentation of 3D models, they are typically validated only on models of high quality and do not possess good generalizability to arbitrary objects. Because the reconstructed 3D models usually lack sharp geometric features and have large noise, unsmooth surfaces, and blurry textures, directly applying 3D segmentation to these models can lead to unsatisfactory results, as presented in Fig. 6.

In this paper, we propose a novel framework to reconstruct a part-aware 3D model from a single-view image, named **Part123**. Given an input image, our method first follows the basic paradigm of multiview diffusion [Liu et al. 2023a; Long et al. 2023a] to generate a set of multiview-consistent images. Instead of recovering the geometry first and then segmenting the shapes in 3D, we propose to utilize the 2D segmentation predicted from multiview images and lift them to 3D space concurrently with the reconstruction process. The 2D segmentation masks are predicted by Segment Anything Model (SAM) [Kirillov et al. 2023], which is a generalizable image segmentation model trained on diverse and large-scale 2D data sources. Based on these 2D representations, we develop



Figure 2: 2D segmentation masks without correspondence and with multi-view inconsistency (highlighted with red boxes). Left: multiview images. Right: 2D segmentation masks from SAM [Kirillov et al. 2023]; different colors indicate different parts, and there is no correspondence between masks across views.

a unified framework based on NeuS [Wang et al. 2021] to jointly reconstruct the 3D model together with its part-aware feature field using contrastive learning. Once the model is trained, a 3D model with segmented parts can be extracted automatically with the help of a simple feature clustering method.

Part123 integrates multiview generation with a 2D segmentation model, seamlessly connecting the process of part-aware 3D reconstruction from a single-view image, exhibiting a set of unique advantages. First, Part123 has a great generalization ability to tackle arbitrary objects thanks to the generalizable 2D segmentation model. By considering part segmentation on 2D images instead of 3D models, it can leverage advanced 2D segmentation models like SAM [Kirillov et al. 2023], while there is no such 3D counterpart due to the relative scarcity of large-scale 3D datasets. Second, 2D segmentation can potentially capture more fine-grained parts due to the rich details embedded in images. Contrarily, segmentation of 3D models usually relies on pre-defined part structures [Hou et al. 2019; Kalogerakis et al. 2017] or distinct geometrical features [Kaick et al. 2014; Lin et al. 2020b], which can be limited to certain object categories or neglect some meaningful parts due to lack of distinguishable geometrical clues. These problems can become more severe when the target 3D model is of low quality like the reconstructed ones. Our method only depends on 2D images and thus will not be affected by the quality of 3D models.

One of the main challenges of Part123 is the uncorrelated and inconsistent 2D segmentation across views. SAM produces segmentation masks without specific categories, thus there are not any explicit correspondences between masks in different views. Moreover, since SAM predicts each individual image, there is no guarantee of the multiview consistency of 2D segmentation. As shown in Fig.2, the head may be a single part or belong to the body when observed from different views. Another problem is how to automatically determine the number of parts without user intervention, which can greatly affect the quality of part-aware models.

To tackle these issues, we introduce contrastive learning into the reconstruction process and learn a 3D feature field for part distinction under the framework of neural radiance fields [Mildenhall et al. 2020; Wang et al. 2021], and we develop an automatic algorithm to determine the part numbers based on multiview SAM predictions. To be specific, a part-segment branch is added to the NeuS [Wang et al. 2021] model, which can output a high-dimensional feature for each 3D point. Such features can be computed for pixel samples with volume rendering technique [Kajiya and Von Herzen 1984]. During training, features corresponding to pixels from the same mask in the same view are optimized to be similar while features from different masks are separated apart. Once the model is trained, part-aware features can be extracted for individual 3D points and

are leveraged for part segmentation with feature clustering. Besides, an effective algorithm is proposed to automatically estimate the number of parts based on multiview 2D segmentations, which is a crucial hyperparameter for feature clustering. A graph is built to search for the connections between different masks in neighboring frames, and connected components can be found to indicate the existence of individual parts. With the combination of part-aware features and automatic determination of part numbers, a 3D model with part segments can thus be reconstructed.

Experiments on the Google Scanned Object dataset [Downs et al. 2022] and real-world images show that our method can produce a 3D model with high-quality part segments on various objects. In addition, we demonstrate some applications with the part-aware models generated by our method, including feature-preserving reconstruction, primitive-based reconstruction, and shape editing. These collectively affirm the effectiveness and generalizability of our method, thereby significantly advancing the integration of single-view 3D reconstruction into practical applications.

2 RELATED WORK

2.1 Single-view Reconstruction

The recent prosperity of diffusion models [Ho et al. 2020; Sohl-Dickstein et al. 2015] has given birth to many new techniques in single-view reconstruction. A large number of methods extend the diffusion framework to 3D generation task [Cheng et al. 2023; Gu et al. 2023a; Jun and Nichol 2023; Karnewar et al. 2023a; Nam et al. 2022; Nichol et al. 2022; Vahdat et al. 2022; Zheng et al. 2023, 2022] to directly produce 3D models. These methods depend on 3D datasets for supervision, but the lack of diverse large-scale 3D data makes it rather difficult to train a generalizable model for arbitrary 3D shapes. Some works thus resort to using 2D multiview images for supervision [Chen et al. 2023; Karnewar et al. 2023b], yet it remains challenging to achieve high-quality reconstruction with strong generalization ability.

Another line of work proposes to utilize 2D diffusion models for 3D generation. DreamFusion [Poole et al. 2022] and SJC [Wang et al. 2023] have pioneered in distilling a pretrained 2D text-to-image diffusion model for text-to-3D synthesis, and this framework is combined with textual inversion [Gal et al. 2022] to enable single-view reconstruction, such as NeuralLift-360 [Xu et al. 2023], RealFusion [Melas-Kyriazi et al. 2023], Make-it-3D [Tang et al. 2023], Magic123 [Qian et al. 2023] and DreamBooth3D [Raj et al. 2023]. In spite of the progress, these methods may fail for certain objects due to the difficulty involved in optimization.

Some other works focus on generating 2D multiview images and use them for 3D reconstruction [Chan et al. 2023; Gu et al. 2023b; Liu et al. 2023b; Long et al. 2023a,b, 2022; Szymanowicz et al. 2023; Tewari et al. 2023; Xiang et al. 2023] by utilizing training images rendered from large-scale 3D datasets like Objaverse [Deitke et al. 2023], and research efforts are taken to improve the multiview consistency of generation results [Liu et al. 2023a; Xie et al. 2023]. Among these methods, SyncDreamer [Liu et al. 2023a] proposes to generate multiview consistent images by synchronizing the diffusion states across different views, and Wonder3D [Long et al. 2023a] produces depth maps along with the RGB images to provide additional geometrical clues for reconstruction.

2.2 Part-Aware 3D Generation

3D models with part-based structures are highly informative for shape processing. With the development of deep generative models and the increasing availability of 3D datasets, many research efforts have been devoted to learning to generate 3D models with part structures. Some methods [Lin et al. 2020a; Niu et al. 2018; Paschalidou et al. 2020] learn to generate primitive-based shape structures from a single image. SDM-NET [Gao et al. 2019] encodes the global structure and detailed geometry of each part separately with two VAEs, and Sagnet [Wu et al. 2019] jointly analyzes the structure and geometry information using an attention mechanism. StructureNet [Mo et al. 2019] models the hierarchical part decomposition with a graph network. PQ-NET [Wu et al. 2020] uses sequential modeling for part assembling and generation. DiffFacto [Nakayama et al. 2023] and SALAD [Koo et al. 2023] introduce diffusion models into part-aware generation tasks for better modeling of structural information. Neural parts [Paschalidou et al. 2021] perform single-view reconstruction by representing 3D models as semantically consistent primitive-based part segments with invertible neural networks. ANISE [Petrov et al. 2023] reconstructs 3D models by assembly part instances that are represented as implicit neural functions. These methods mainly depend on annotated 3D datasets for supervision, yet the limited diversity of existing 3D datasets is insufficient to train a generalizable model. Moreover, as they usually rely on pre-defined structures of certain objects, these methods are often category-specific and only support certain kinds of shapes.

2.3 3D Segmentation

3D segmentation has been a long-standing problem in many applications, such as mesh editing [Hertz et al. 2022], skeleton generation [Dou et al. 2022; Lin et al. 2021], and motion synthesis [Dou et al. 2023; Tevet et al. 2022; Zhou et al. 2023]. Some methods focus on the analysis of geometrical properties to segment 3D shapes based on some rules [Chen et al. 2009], which usually assumes that a 3D model can be approximately decomposed into some convex parts. Some representative methods are built upon weakly convex decomposition [Asafi et al. 2013; Kaick et al. 2014], shape diameter function [Shapira et al. 2008], random walks [Lai et al. 2008], random cuts [Golovinskiy and Funkhouser 2008], Kmeans [Shlafman et al. 2002], primitive fitting [Attene et al. 2006], core extraction [Katz et al. 2005] and median axis [Lin et al. 2020b]. Another group of methods learn the 3D segmentation models with supervision of pre-defined labels, which include different components with semantic meanings [Guo et al. 2015; Hou et al. 2019; Kalogerakis et al. 2017, 2010; Xu et al. 2017]. These methods are limited to the pre-defined categories and can hardly be applied to arbitrary objects. Some other methods employ unsupervised learning to discover the intrinsic geometry of 3D shapes without pre-defined labels [Shu et al. 2016; Sun and Zou 2019; Tulsiani et al. 2017], yet they still require large-scale training datasets and are category-specific.

With the advent of vision-language models, such as CLIP [Radford et al. 2021], and the generalizable image segmentation model like SAM [Kirillov et al. 2023], some works have resorted to lifting 2D segmentation to 3D space. OpenMask3D [Takmaz et al. 2023] aggregates CLIP features from multiview images for object

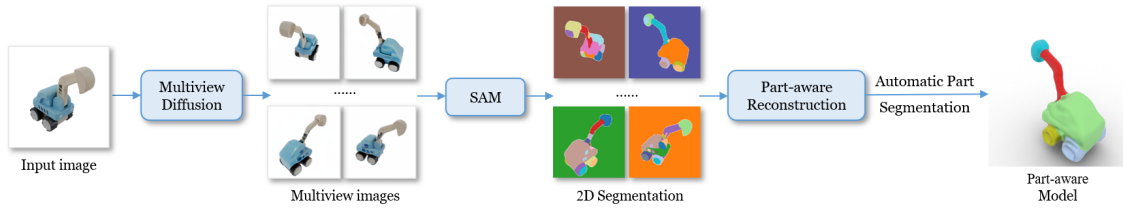


Figure 3: Overall framework of our method, Part123. Our method takes a single-view image as input and generates its 3D model with segmented part components. For a single-view input, we first generate its multiview images using multiview diffusion. Then their 2D segmentation masks are predicted with a generalizable 2D image segmentation model, SAM, and part-aware reconstruction is conducted based on these 2D segmentations. Finally, the reconstructed model with part segments is built using an automatic algorithm. Note: for the "2D Segmentation" and "Part-aware Model", different colors indicate different parts.

instances to perform open-vocabulary scene understanding. ConceptFusion [Jatavallabhula et al. 2023] incorporates multimodal representations into the 3D mapping framework to build open-set 3D maps. SA3D [Cen et al. 2023] proposes an iterative cross-view framework to project 2D segmentation masks onto 3D space based on the density distribution of a trained NeRF model [Mildenhall et al. 2020], and it can generate a 3D segmentation mask for a target object at a time. Semantic image features can also be distilled into a 3D field under a NeRF [Mildenhall et al. 2020] framework to enable scene editing in a radiance field [Kobayashi et al. 2022]. SAM3D [Yang et al. 2023] develops a bidirectional merging approach to fuse multiview 2D segmentation masks in 3D space to get the 3D segmentation for a whole scene. PartSLIP [Liu et al. 2023d] also introduces a 3D fusion algorithm to lift 2D segmentations to target 3D point clouds. In addition, as it is built upon GLIP [Li et al. 2022], a large image-language model, it also proposes to finetune the model for better text prompt understanding and multiview feature aggregation. These methods serve as competitive tools for generalizable 3D segmentation by taking advantage of the generalization capacity of 2D segmentation models, while 3D segmentation methods have limited generalization due to the scarcity of 3D data compared to their 2D image counterparts. Unlike most existing methods, our work takes a different route from explicit fusion by using contrastive learning to integrate the perception of structures into reconstruction, which is the first such attempt within the context of single-view reconstruction.

3 METHODS

The overall framework of Part123 is presented in Fig. 3. Our method takes a single-view image as input and generates a corresponding 3D model with segmented parts. Given an input image of a target object, a multiview diffusion model is first applied to generate a set of multiview images surrounding the object (Sec. 3.1). We then adopt the generalizable image segmentation model, SAM [Kirillov et al. 2023], to obtain the 2D segmentation results for these multiview images, which are used to reconstruct the part-aware 3D model. Next, a neural rendering framework [Mildenhall et al. 2020] is leveraged for 3D reconstruction, where a part-segment branch based on contrastive learning is introduced into NeuS [Wang et al. 2021] to learn a part-aware feature space (Sec. 3.2). Finally, we propose an algorithm to automatically determine the part number and extract the segments of the shape (Sec. 3.3).

3.1 Multiview Diffusion

Given a single-view image of an object, multiview diffusion models can generate the corresponding multiview consistent images for 3D reconstruction. In this paper, we use SyncDreamer [Liu et al. 2023a] to generate multiview images, which yields $N=16$ images at fixed viewpoints. The theory of multiview diffusion is built upon diffusion models [Ho et al. 2020; Sohl-Dickstein et al. 2015], which models the distribution of data z_0 and a sequence of latent variables $z_{1:T} := z_1, \dots, z_T$ as a Markov chain. Specifically, in the forward process of a diffusion model, random noises are gradually added to data z_0 until it becomes completely Gaussian noise. This process can be formulated as $q(z_{1:T}|z_0) = \prod_{t=1}^T q(z_t|z_{t-1}) = \prod_{t=1}^T N(z_t; \sqrt{\alpha_t}z_{t-1}, (1 - \alpha_t)\mathbf{I})$, where α_t is a time-dependent constant for noise schedule. The reverse process generates data by a denoising process starting from z_T sampled from $N(0, \mathbf{I})$, and the joint distribution of z_0 and $z_{1:T}$ is $p(z_{0:T}) = p(z_T) \prod_{t=1}^T p_\theta(z_{t-1}|z_t)$, where $p_\theta(z_{t-1}|z_t) = N(z_{t-1}; \mu_\theta(z_t, t), \sigma_t^2 \mathbf{I})$, $\mu_\theta(z_t, t)$ is learnable by networks and σ_t is a constant related to α_t .

To enhance the multiview consistency of generated images, multiview diffusion models take a step further and propose to model the joint distribution of all views. The forward process still adds noises independently to every single view, and the reverse process is an extension of the general denoising process: $p(z_{0:T}^{(1:N)}) = p(z_T^{(1:N)}) \prod_{t=1}^T p_\theta(z_{t-1}^{(1:N)}|z_t^{(1:N)})$, where N is the number of views. Starting from this formulation, SyncDreamer [Liu et al. 2023a] adopts a 3D spatial volume and attention mechanism to correlate features from all views during the generation process.

3.2 Part-Aware Reconstruction with Contrastive Learning

With the generated multiview images, we propose to perform part-aware image-based reconstruction by utilizing 2D segmentation results predicted from these images. We use the pre-trained model SAM [Kirillov et al. 2023] to obtain the 2D segmentation masks on each view. SAM is a generalizable foundation model for image segmentation, and it can automatically generate instance segmentation masks for an entire image. Note that the mask produced by SAM is semantic-agnostic, and thus the correspondence between masks in different views is unavailable. Moreover, due to the appearance changes across views, segmentation of each part can be inconsistent in different views, as shown in Fig. 2 and Fig. 5.

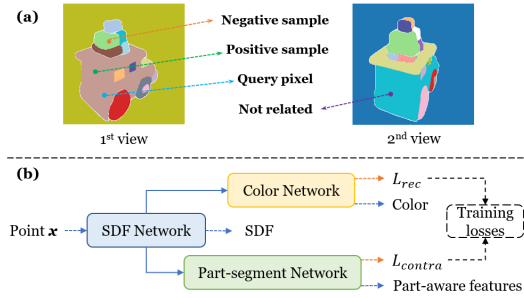


Figure 4: (a) Illustration on the sampling strategy for contrastive learning. For each query pixel, its positive sample is selected from the same segmentation mask and its negative sample is from a different mask in the same view. There is no restriction between pixels in different views. (b) The proposed part-aware NeuS network with a part-segment branch. Training losses can be calculated using pixel-level outputs computed with volume rendering through all sampled points along the rays.

Consequently, instead of directly aggregating the 2D segmentation labels, we integrate the part-aware operations into the reconstruction process. Specifically, we introduce an additional branch into the neural rendering framework of NeuS [Wang et al. 2021] to construct a feature space. NeuS is a neural surface reconstruction approach based on multiview images. It outputs an SDF (signed distance function) value and a color value for each 3D point, representing the geometry and appearance properties respectively. Both values are encoded by neural networks. To effectively learn the part-aware features based on the 2D segmentation masks, we propose to use contrastive learning to distinguish the features of different parts when optimizing the geometry of individual views. This approach not only allows for part-aware learning to fully capture the implicit features of geometry and appearance, but it also obviates the need to consider the consistency and correlation of masks across multiple views. Even though we only impose constraints on the features of parts belonging to the same view, the optimization process of NeuS model will globally correlate the multiview information, hence the consistency across different views is naturally achieved.

As shown in Fig. 4 (b), for a given point x , the part-segment network takes as input the intermediate feature from the SDF network and outputs a part-aware feature F_x with N_c channels at this point. The part-aware feature of a certain ray corresponding to a sampled image pixel can thus be calculated with volume rendering [Kajiya and Von Herzen 1984] by accumulating through all sampled points on this ray. In every training step, we first sample N_q pixels as queries. For every query pixel q , we then sample N_{pos} pixels from the same segmentation mask with q as its corresponding positive samples, and sample N_{neg} pixels from different masks within the same view of q as its negative samples (see Fig. 4 (a)). Note that we do not impose any restrictions on the pixels from different views, as there are no relationships between their segmentation masks. Under the contrastive learning framework, the ray-based features of query and positive pixel samples are optimized to be similar, while features of query and negative pixel samples are driven far from each other.

For the training process, InfoNCE loss [Oord et al. 2018] is adopted for contrastive learning: $L_{contra} = -\mathbb{E}[\log \frac{f(x_q, x_{pos})}{\sum_{n=1}^N f(x_q, x_n)}]$, where N is the number of samples, and f is a scoring function related to mutual information optimization. The overall loss function is defined as $L = L_{rec} + \alpha L_{contra}$, where L_{rec} is the reconstruction loss used in the vanilla NeuS model related to multiview images, as presented in Fig. 4 (b). α is the weight for contrastive loss and is experimentally set to 0.02, as we noticed that a large value may lead to geometrical artifacts. The part-aware NeuS model is trained for 2k steps.

3.3 Automatic Part Segmentation

Once the NeuS model is trained, the mesh of the corresponding 3D model can be extracted from the learned neural field with marching cube [Lorensen and Cline 1987]. Then, there is another important step to obtain the part segments from it along with the reconstructed mesh. For each vertex of the mesh, we can obtain their part-aware features from the part-segment branch. These per-vertex features are then used for part segmentation, where we use KMeans [Lloyd 1982] to get M clusters corresponding to M segmented parts.

The number of clusters and the initial centers play a vital role in the performance of KMean clustering. Although the part-aware feature space we have learned supports users to manually specify prompts or part numbers for segmentation, considering the significant advantages of a fully automatic algorithm in real applications, we thus develop an algorithm to automatically figure out these reasonable hyperparameters and generate high-quality part segmentation results.

There are two main steps involved in the automatic algorithm. First, we introduce a graph-based method to estimate the desired part number based on the correspondence among multiview 2D segmentation masks. Every segmentation mask is represented by a vertex in the graph, and an edge will be added if two masks are estimated to belong to the same part in the 3D model. Once the graph is built, we can search for connected components in the graph, and each component will correspond to a part segment. In this way, only masks within neighboring frames need to be considered for local connectivity. For a source mask M_a from the k_{th} view I_k and a target mask M_b from the $(k+1)_{th}$ view I_{k+1} , we project M_a onto I_{k+1} to obtain M_{ab} according to the depth values derived from the NeuS model, and occlusions can also be detected based on depths. If the overlapping ratios between (M_{ab}, M_b) and (M_{ab}, M_a) are both above a certain threshold τ , we decide that M_a and M_b correspond to the same part and add an edge between them. By iterating over the N frames, we can finally build a complete graph to find the number of parts. In addition, we choose an internal pixel from the largest mask of each part as a reference pixel, which is approximately at the mask center, and use its corresponding 3D point as one of the KMeans initial centers.

The second step aims to select the best part-segment result from those generated with different overlapping ratios within a specified range. By setting the overlapping ratio to different values in the first step, we can obtain multiple segmentation results with different numbers of parts. In particular, a larger ratio value will impose harder restrictions for two masks to be detected as the same part, thus leading to more segmented parts. We experimentally

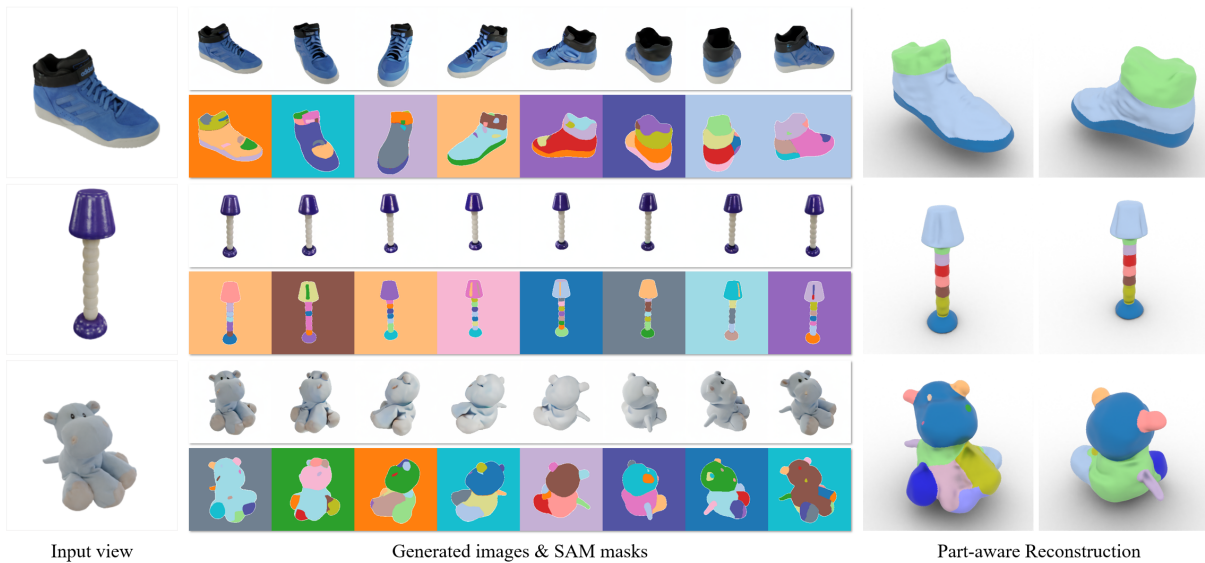


Figure 5: Qualitative results of part-aware reconstruction by our method, based on 2D segmentation masks with high inconsistency across views. For each object, we show the input single-view image, the generated multiview images along with their corresponding 2D segmentation masks, and the part-aware 3D reconstruction model. Our method can produce 3D models with high-quality part segments in spite of the inconsistent multiview segmentations.

sample the overlapping ratio in the range of 0.2~0.7. We further select an output with better overall quality according to an unsupervised metric for clustering evaluation, Davies-Bouldin score (DB-score) [Davies and Bouldin 1979], which measures the similarity between all clusters, and a lower value indicates a better clustering result with more distinctive segmented parts. The part-segment model with the lowest DB-score is thus given as the final output of 3D reconstruction generated by Part123. We can further distinguish the geometrically separated parts according to the connectivity of the labels on the mesh.

4 EXPERIMENTS

4.1 Dataset

We follow the practice of previous works [Liu et al. 2023a; Long et al. 2023a] to use the Google Scanned Objects (GSO) dataset [Downs et al. 2022] to evaluate the performance of our method. To be specific, we select testing cases from the GSO dataset with various kinds of objects, and an input image of size 256×256 is rendered for each object with an elevation angle of 30° , which is a default parameter used in SyncDreamer [Liu et al. 2023a].

4.2 Results and Comparisons

We compare the reconstruction quality of our method with four state-of-the-art approaches for single-view reconstruction, including Point-E [Nichol et al. 2022], Shap-E [Jun and Nichol 2023], One-2-3-45 [Liu et al. 2023c] and SyncDreamer [Liu et al. 2023a]. Point-E and Shap-E directly generate 3D models in the form of point clouds or implicit functions. One-2-3-45 performs 3D reconstruction based on the generated images of Zero123 [Liu et al. 2023b]. To evaluate the quality of reconstructed models, we adopt two commonly used metrics, Chamfer Distances and Volume IoU, which

measure the difference between the reconstructed and ground truth shapes. Quantitative results are shown in Table 1. The reconstruction quality of our approach is comparable to the baseline method, SyncDreamer, and greatly outperforms the other three methods. This indicates that our method can achieve part-aware reconstruction without any deterioration of the reconstruction quality.

We further demonstrate results for part-aware reconstruction in Fig. 5 and Fig. 6. Fig. 5 shows the 3D reconstruction with part segments generated by our method, together with the 2D segmentation masks of multiview images. It can be seen that there exist a large amount of inconsistent 2D segmentations across different views, and our method can still produce high-quality part segments by preserving the most distinct parts and neglecting the parts corresponding to noisy masks. We also compare the part segmentation results of our reconstructed models with some state-of-the-art methods, including SAM3D [Yang et al. 2023], WCseg [Kaick et al. 2014], and SEG-MAT [Lin et al. 2020b]. SAM3D [Yang et al. 2023] is a representative approach to generalizable 3D segmentation depending on SAM [Kirillov et al. 2023], which lifts 2D segmentation masks to the input 3D models using an iterative merging algorithm. WCseg [Kaick et al. 2014] and SEG-MAT [Lin et al. 2020b] are two methods based on geometrical analysis. Note that we do not compare with learning-based approaches for semantic segmentation, since they are restricted to certain object categories rather than the arbitrary objects used in our method. Comparison results are shown in Fig. 6, and we use the reconstructed models from NeuS [Wang et al. 2021] as the inputs to the other three methods. The results of SAM3D [Yang et al. 2023] suffer from unclear boundaries between different parts and tend to lose fine-grained part segments due to its inter-frame fusion strategies without considering the global structures. The two geometry-based approaches show much clearer



Figure 6: Comparison of 3D part segmentation with state-of-the-art methods, including SAM3D [Yang et al. 2023], WCSEg [Kaick et al. 2014] and SEG-MAT [Lin et al. 2020b]. Our method generates high-quality part segments with clear boundaries and meaningful parts, while other methods show inferior results due to noisy boundaries or missing parts.

Table 1: Quantitative comparison with state-of-the-art methods for single-view reconstruction in terms of the reconstruction quality.

Methods	Chamfer Dist. ↓	Volume IoU ↑
Point-E [Nichol et al. 2022]	0.0541	0.2598
Shap-E [Jun and Nichol 2023]	0.0532	0.3275
One-2-3-45 [Liu et al. 2023c]	0.0870	0.2906
SyncDreamer [Liu et al. 2023a]	0.0359	0.4876
Ours	0.0354	0.4943

boundaries than SAM3D but struggle to produce meaningful parts. In contrast to these results, our method can produce high-quality and meaningful part segments with clear boundaries. In addition, it can be seen that our method can segment the teapot lid as a single part, while WCSEg and SEG-MAT fail to do so since they mainly depend on convexity clues and cannot distinguish parts with similar geometrical properties. This phenomenon further validates the merits of incorporating 2D image segmentation to help with 3D segmentation. Results generated by our method on more testing examples are presented in Fig. 9.

We also conduct a user study to evaluate how well the segmentation results align with human perception, considering that there is no clear quantitative evaluation standard for the generic segmentation task. Specifically, we sample 22 testing cases and invite 46 participants to join the study. For each case, participants are asked to select the best segmentation result generated by four methods. The quantitative comparison is presented in Table 2. Our method outperforms the other three approaches by a large margin, indicating that our segmentation results better conform to the human perception of 3D shape structures.

5 ANALYSIS AND DISCUSSIONS

In this section, we conduct a set of experiments to verify the efficacy of our designs and give some in-depth analysis of our method.

Table 2: User study to evaluate the segmentation quality, in comparison with WCSEg [Kaick et al. 2014], SEG-MAT [Lin et al. 2020b] and SAM3D [Yang et al. 2023].

Methods	WCSEg	SEG-MAT	SAM3D	Ours
Percent. of Favorite ↑	7.2%	9.4%	10.1%	73.3%

5.1 Overlapping Ratio

We show the part-aware 3D reconstruction results produced with different overlapping ratios in the left image of Fig. 7. It can be seen that a larger value tends to produce more fine-grained part segments in the reconstructed models. On the other hand, a smaller value may potentially lead to the under-segmentation of some local parts and merge some similar parts, like the feet of the boy in the 1st case. This phenomenon helps to justify the necessity of choosing an appropriate part number to generate a final output, as proposed in our automatic algorithm. In practice, users can also manually select a proper value of overlapping ratio according to their specific application scenarios, since different applications often have different requirements on the levels of segmented structures.

5.2 KMeans Initialization

We additionally justify the efficacy of using the estimated mask centers as the initial centers of KMeans clustering in the right image of Fig. 7. Note that for the experiment without initial centers, we still use the same estimated number of parts with the same overlapping ratio, but only ignore the estimated part centers and use the default random initialization of KMeans. It can be seen that clustering without using the estimated initial centers can sometimes lead to unreasonable part segments, like the redundant parts between the seat and back of the sofa in the 1st case, and the separated part on a single side of the refrigerator in the 2nd case. On the contrary, results generated with estimated initial centers are more robust to generate meaningful part segments.

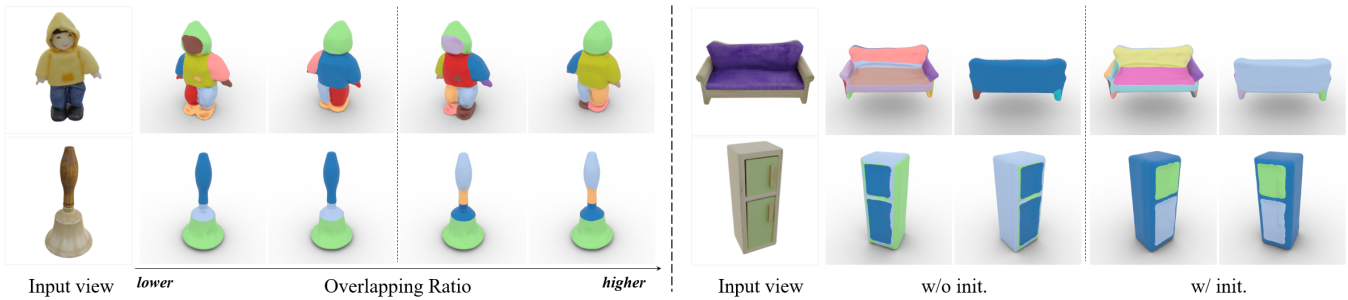


Figure 7: (a) Left: Comparison of part-aware reconstructions with two different overlapping ratios used in the automatic algorithm, where a larger value leads to more fine-grained part segments. (b) Right: Comparison of part-aware reconstructions with and without initialization of clustering centers for KMeans. By initializing the KMeans centers using estimated mask centers, Part123 can generate meaningful part segments more robustly than the default random initialization of KMeans.

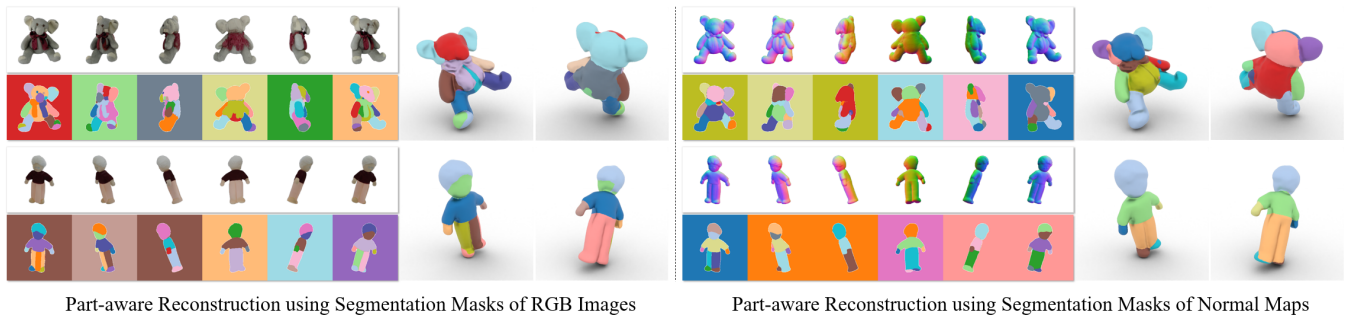


Figure 8: Results of part-aware reconstruction based on another multiview diffusion backbone, Wonder3D [Long et al. 2023a]. Wonder3D can generate multiview images along with their normal maps, and we show the reconstruction results using 2D segmentation masks of either RGB images or their normal maps. Our method can perform robustly and generate reasonable part-segmented reconstructions based on 2D segmentations of RGB images / normal maps, showing its generalization ability to different backbones and different image domains.

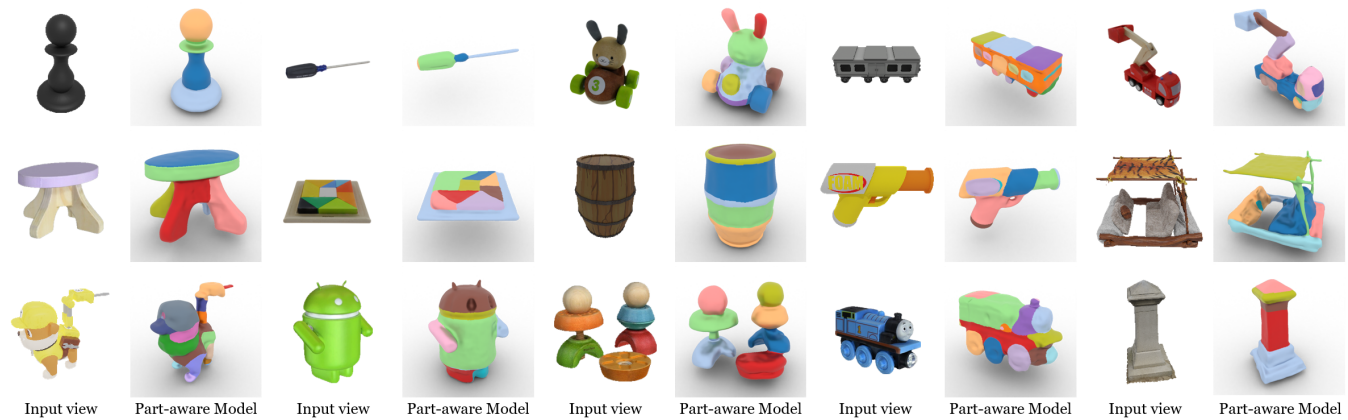


Figure 9: More results of part-aware reconstruction generated by our method.

5.3 Amount of Multi-view Images

To validate the robustness of our method to the number of multiview images, we conduct experiments with different numbers of multiview images by uniformly sampling from the 16 images generated by SyncDreamer [Liu et al. 2023a]. Qualitative results are shown in

Fig. 10. Our method performs robustly with a decreasing number of multiview images for part-aware reconstruction and yields 3D models with persistent quality of part segmentations. This helps to prove the effectiveness of employing part-aware reconstruction based on 2D segmentation masks using contrastive learning.

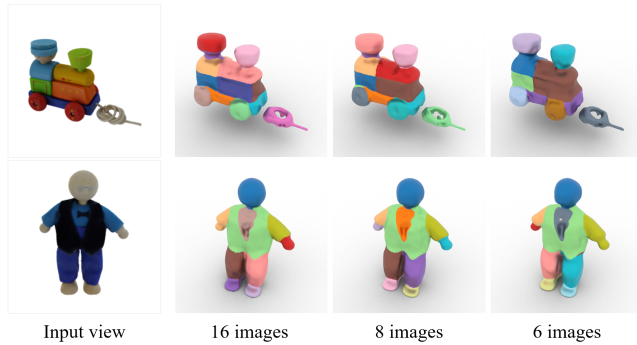


Figure 10: Part-aware reconstruction using various numbers of multi-view images. All images are generated by SyncDreamer, and we uniformly sample from the original image set for the experiments with 8 and 6 images. With a decreasing number of multiview images, Part123 can perform part-aware 3D reconstruction with persistent part segmentation results, even with as few as six views.

5.4 Different Backbones

We show the robustness of our method towards different generative models and 2D representations from different domains. We present part-aware reconstructions based on Wonder3D [Long et al. 2023a], which is another state-of-the-art method for single-view reconstruction using multiview diffusion. Wonder3D simultaneously generates multiview images and their corresponding normal maps, and the latter provides additional geometrical supervision for image-based reconstruction. We show the reconstruction results based on the segmentation masks of RGB images and normal maps in Fig. 8. Our method performs consistently with a different backbone, and thanks to the generalization ability of SAM [Kirillov et al. 2023], our method can still generate reasonable part segments using the 2D segmentation of normal maps. We also observe that, since RGB images and normal maps demonstrate different patterns, where the former can be more affected by textures and the latter focus more on geometrical properties, the part segments produced by the two kinds of segmentation will accordingly lead to differences in some local parts.

6 APPLICATIONS

With the reconstructed part-aware 3D models at hand, this section demonstrates some interesting applications of shape processing by utilizing the information on part segmentation.

6.1 Feature-preserving Reconstruction

It has long been a demanding task for 3D reconstruction to preserve sharp features while smoothing insignificant noises. For reconstructed models that usually lack sharp features, it can be rather hard to preserve or recover sharp edges with geometrical feature analysis. We demonstrate that our method provides an easier solution to this problem by combining with mesh filtering techniques [Zhang et al. 2015; Zheng et al. 2011]. Comparison between the mesh filtering results of reconstructed models with and without the guidance of part segments is presented in Fig. 11.

Under the guidance of part segments, where additional information about part boundaries serves as hints on sharp features that should be preserved during the filtering process, the mesh filtering method [Zheng et al. 2011] can recover sharper edges near the part boundaries, while those processed without part-aware information fail to figure out these sharp features and lead to over-smoothed reconstruction.

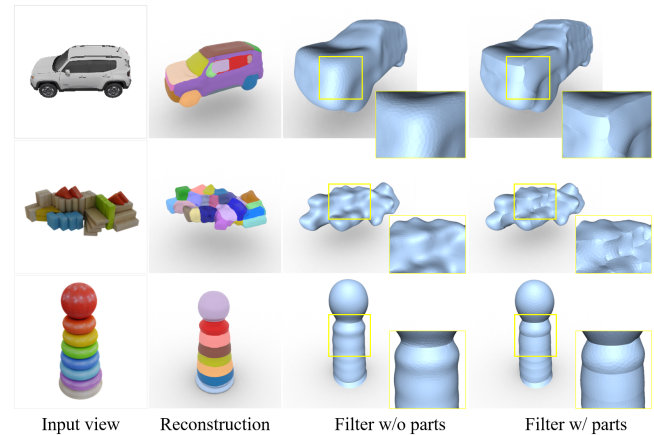


Figure 11: Results of feature-preserving reconstruction based on part segments. When combined with mesh filtering, the knowledge of part segments provided by our method helps to recover much sharper details compared with meshes that are processed without part-aware clues.

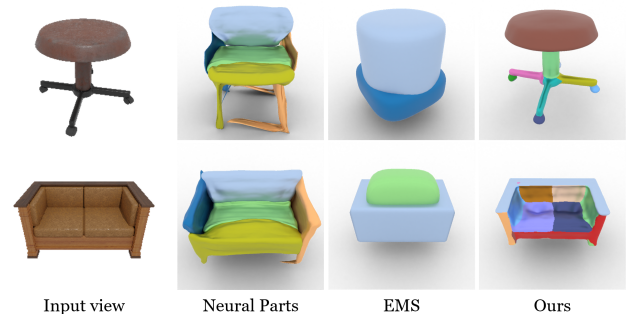


Figure 12: Visual comparison with two primitive-based part-aware methods, Neural Parts [Paschalidou et al. 2021] and EMS [Liu et al. 2022]. The results of Neural Parts and EMS struggle for various real-world objects, and are inferior to our results in terms of the perception of part structures.

6.2 Primitive-based Reconstruction

Geometrical primitives [Kaiser et al. 2019] play a critical role in understanding the intrinsic structures of 3D shapes. With a 3D model with part segments, one can easily build the primitive-based abstraction of the whole shape by fitting each part with a primitive. In this

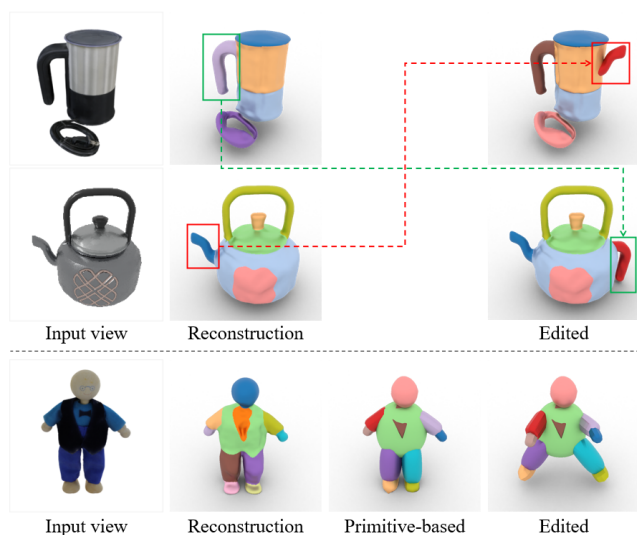


Figure 13: Results of shape editing based on the awareness of part segments.

paper, we try to fit each part with superquadric primitives [Paschalidou et al. 2019], and we use EMS [Liu et al. 2022] to estimate the superquadric parameters of each part. We additionally apply shape deformation [Sumner and Popović 2004] to each fitted part to make it align more closely to the original geometry. Results are presented in Fig. 1. The reconstructed shapes can be well fitted into approximate superquadric components with a higher level abstraction, showing the effectiveness of our reconstructed part-aware models for the downstream task of primitive fitting. We also compare our reconstruction results with two primitive-based part-aware methods in Fig. 12, where Neural Parts [Paschalidou et al. 2021] perform part-aware reconstruction from a single image like our method, and EMS [Liu et al. 2022] can take a reconstructed 3D model as input and fit it with multiple parts using superquadric primitives. Our method generates better results in terms of the quality of part segments.

6.3 Shape Editing

We demonstrate the results of 3D shape editing based on the part-aware models in Fig. 13. With the information of part structures, we can easily edit the reconstructed models with parts from other reference models, or change the character’s pose by adjusting its body parts. For the latter task, we first fit the 3D model with multiple superquadric primitives and then edit the poses of some articulated parts. This task can be difficult for a reconstructed model without any structural information, while our part-aware model makes this process much easier and more straightforward.

7 CONCLUSION

This paper proposes Part123, a novel framework for part-aware 3D model reconstruction from a single-view image. Part123 follows the multiview diffusion paradigm to generate multiview images for 3D reconstruction and leverages a generalizable 2D segmentation

model to predict 2D segmentations of multiview images. To lift the 2D segmentations to 3D models and handle the inconsistency of multiview segmentation, contrastive learning is introduced into NeuS to learn a part-aware feature space. An automatic algorithm is proposed to estimate the appropriate part numbers to generate the final part-segmented 3D models.

ACKNOWLEDGMENTS

The research of this work is partially funded by the Innovation and Technology Commission of the HKSAR Government under the InnoHK initiative and Ref. T45-205/21-N of Hong Kong RGC.

REFERENCES

- Shmuel Asafi, Avi Goren, and Daniel Cohen-Or. 2013. Weak convex decomposition by lines-of-sight. In *Computer graphics forum*, Vol. 32. Wiley Online Library, 23–31.
- Marco Attene, Bianca Falcidieno, and Michela Spagnuolo. 2006. Hierarchical mesh segmentation based on fitting primitives. *The Visual Computer* 22 (2006), 181–193.
- Jiazhong Cen, Zanwei Zhou, Jiemin Fang, Chen Yang, Wei Shen, Lingxi Xie, Xiaopeng Zhang, and Qi Tian. 2023. Segment Anything in 3D with NeRFs. In *NeurIPS*.
- Eric R Chan, Koki Nagano, Matthew A Chan, Alexander W Bergman, Jeong Joon Park, Axel Levy, Miika Aittala, Shalini De Mello, Tero Karras, and Gordon Wetzstein. 2023. Generative novel view synthesis with 3d-aware diffusion models. *arXiv preprint arXiv:2304.02602* (2023).
- Hansheng Chen, Jiatao Gu, Anpei Chen, Wei Tian, Zhuowen Tu, Lingjie Liu, and Hao Su. 2023. Single-Stage Diffusion NeRF: A Unified Approach to 3D Generation and Reconstruction. *arXiv preprint arXiv:2304.06714* (2023).
- Xiaobai Chen, Aleksey Golovinskiy, and Thomas Funkhouser. 2009. A benchmark for 3D mesh segmentation. *Acm transactions on graphics (tog)* 28, 3 (2009), 1–12.
- Yen-Chi Cheng, Hsin-Ying Lee, Sergey Tulyakov, Alexander G Schwing, and Liang-Yan Gui. 2023. Sdfusion: Multimodal 3d shape completion, reconstruction, and generation. In *Proceedings of the IEEE/CVF Conference on Computer Vision and Pattern Recognition*. 4456–4465.
- David L. Davies and Donald W. Bouldin. 1979. A Cluster Separation Measure. *IEEE Trans. Pattern Anal. Mach. Intell.* 1, 2 (1979), 224–227.
- Matt Deitke, Dustin Schwenk, Jordi Salvador, Luca Weihs, Oscar Michel, Eli VanderBilt, Ludwig Schmidt, Kiana Ehsani, Aniruddha Kembhavi, and Ali Farhadi. 2023. Objaverse: A universe of annotated 3d objects. In *Proceedings of the IEEE/CVF Conference on Computer Vision and Pattern Recognition*. 13142–13153.
- Zhiyang Dou, Xuelin Chen, Qingnan Fan, Taku Komura, and Wenping Wang. 2023. C-ase: Learning conditional adversarial skill embeddings for physics-based characters. In *SIGGRAPH Asia 2023 Conference Papers*. 1–11.
- Zhiyang Dou, Cheng Lin, Rui Xu, Lei Yang, Shiqing Xin, Taku Komura, and Wenping Wang. 2022. Coverage axis: Inner point selection for 3d shape skeletonization. In *Computer Graphics Forum*, Vol. 41. Wiley Online Library, 419–432.
- Laura Downs, Anthony Francis, Nate Koenig, Brandon Kinman, Ryan Hickman, Krista Reymann, Thomas B McHugh, and Vincent Vanhoucke. 2022. Google scanned objects: A high-quality dataset of 3d scanned household items. In *2022 International Conference on Robotics and Automation (ICRA)*. IEEE, 2553–2560.
- Alfredo Ferreira, Simone Marini, Marco Attene, Manuel J Fonseca, Michela Spagnuolo, Joaquim A Jorge, and Bianca Falcidieno. 2010. Thesaurus-based 3D object retrieval with part-in-whole matching. *International Journal of Computer Vision* 89 (2010), 327–347.
- Thomas Funkhouser, Michael Kazhdan, Philip Shilane, Patrick Min, William Kiefer, Ayellet Tal, Szymon Rusinkiewicz, and David Dobkin. 2004. Modeling by example. *ACM transactions on graphics (TOG)* 23, 3 (2004), 652–663.
- Rinon Gal, Yuval Alaluf, Yuval Atzmon, Or Patashnik, Amit H Bermano, Gal Chechik, and Daniel Cohen-Or. 2022. An image is worth one word: Personalizing text-to-image generation using textual inversion. *arXiv preprint arXiv:2208.01618* (2022).
- Lin Gao, Jie Yang, Tong Wu, Yu-Jie Yuan, Hongbo Fu, Yu-Kun Lai, and Hao Zhang. 2019. SDM-NET: Deep generative network for structured deformable mesh. *ACM Transactions on Graphics (TOG)* 38, 6 (2019), 1–15.
- Aleksey Golovinskiy and Thomas Funkhouser. 2008. Randomized cuts for 3D mesh analysis. In *ACM SIGGRAPH Asia 2008 papers*. 1–12.
- Jiatao Gu, Qingzhe Gao, Shuangfei Zhai, Baoquan Chen, Lingjie Liu, and Josh Susskind. 2023a. Learning Controllable 3D Diffusion Models from Single-view Images. *arXiv preprint arXiv:2304.06700* (2023).
- Jiatao Gu, Alex Trevithick, Kai-En Lin, Joshua M Susskind, Christian Theobalt, Lingjie Liu, and Ravi Ramamoorthi. 2023b. Nerfdiff: Single-image view synthesis with nerf-guided distillation from 3d-aware diffusion. In *International Conference on Machine Learning*. PMLR, 11808–11826.
- Kan Guo, Dongqing Zou, and Xiaowu Chen. 2015. 3D Mesh Labeling via Deep Convolutional Neural Networks. *ACM Trans. Graph.* 35, 1 (2015), 3:1–3:12.

- Amir Hertz, Or Perel, Raja Giryes, Olga Sorkine-Hornung, and Daniel Cohen-Or. 2022. Spaghetti: Editing implicit shapes through part aware generation. *ACM Transactions on Graphics (TOG)* 41, 4 (2022), 1–20.
- Jonathan Ho, Ajay Jain, and Pieter Abbeel. 2020. Denoising diffusion probabilistic models. *Advances in neural information processing systems* 33 (2020), 6840–6851.
- Ji Hou, Angela Dai, and Matthias Nießner. 2019. 3d-sis: 3d semantic instance segmentation of rgb-d scans. In *Proceedings of the IEEE/CVF conference on computer vision and pattern recognition*. 4421–4430.
- Krishna Murthy Jatavallabhula, Alihusein Kuwajerwala, Qiao Gu, Mohd Omama, Tao Chen, Alaa Maalouf, Shuang Li, Ganesh Iyer, Soroush Saryazdi, Nikhil Keetha, et al. 2023. Conceptfusion: Open-set multimodal 3d mapping. *arXiv preprint arXiv:2302.07241* (2023).
- Zhongping Ji, Ligang Liu, Zhonggui Chen, and Guojin Wang. 2006. Easy mesh cutting. In *Computer Graphics Forum*, Vol. 25. Wiley Online Library, 283–291.
- Heewoo Jun and Alex Nichol. 2023. Shape-e: Generating conditional 3d implicit functions. *arXiv preprint arXiv:2305.02463* (2023).
- Oliver Van Kaick, Noa Fish, Yanir Kleiman, Shmuel Asafi, and Daniel Cohen-Or. 2014. Shape segmentation by approximate convexity analysis. *ACM Transactions on Graphics (TOG)* 34, 1 (2014), 1–11.
- Adrien Kaiser, José Alonso Ybáñez Zepeda, and Tamy Boubekeur. 2019. A Survey of Simple Geometric Primitives Detection Methods for Captured 3D Data. *Comput. Graph. Forum* 38, 1 (2019), 167–196.
- James T Kajiya and Brian P Von Herzen. 1984. Ray tracing volume densities. *ACM SIGGRAPH computer graphics* 18, 3 (1984), 165–174.
- Evangelos Kalogerakis, Melinos Averkiou, Subhransu Maji, and Siddhartha Chaudhuri. 2017. 3D shape segmentation with projective convolutional networks. In *proceedings of the IEEE conference on computer vision and pattern recognition*. 3779–3788.
- Evangelos Kalogerakis, Aaron Hertzmann, and Karan Singh. 2010. Learning 3D mesh segmentation and labeling. *ACM Trans. Graph.* 29, 4 (2010), 102:1–102:12.
- Animesh Karnewar, Niloy J Mitra, Andrea Vedaldi, and David Novotny. 2023a. Holofusion: Towards photo-realistic 3d generative modeling. In *Proceedings of the IEEE/CVF International Conference on Computer Vision*. 22976–22985.
- Animesh Karnewar, Andrea Vedaldi, David Novotny, and Niloy J Mitra. 2023b. Holodiffusion: Training a 3D diffusion model using 2D images. In *Proceedings of the IEEE/CVF Conference on Computer Vision and Pattern Recognition*. 18423–18433.
- Sagi Katz, George Leifman, and Ayellet Tal. 2005. Mesh segmentation using feature point and core extraction. *The Visual Computer* 21 (2005), 649–658.
- Alexander Kirillov, Eric Mintun, Nikhila Ravi, Hanzi Mao, Chloe Rolland, Laura Gustafson, Tete Xiao, Spencer Whitehead, Alexander C. Berg, Wan-Yen Lo, Piotr Dollár, and Ross Girshick. 2023. Segment Anything. *arXiv:2304.02643* (2023).
- Sosuke Kobayashi, Eiichi Matsumoto, and Vincent Sitzmann. 2022. Decomposing nerf for editing via feature field distillation. *Advances in Neural Information Processing Systems* 35 (2022), 23311–23330.
- Juil Koo, Seungwoo Yoo, Minh Hieu Nguyen, and Minhyuk Sung. 2023. Salad: Part-level latent diffusion for 3d shape generation and manipulation. In *Proceedings of the IEEE/CVF International Conference on Computer Vision*. 14441–14451.
- Yu-Kun Lai, Shi-Min Hu, Ralph R Martin, and Paul L Rosin. 2008. Fast mesh segmentation using random walks. In *Proceedings of the 2008 ACM symposium on Solid and physical modeling*. 183–191.
- Bruno Lévy, Sylvain Petitjean, Nicolas Ray, and Jérôme Maillot. 2002. Least Squares Conformal Maps for Automatic Texture Atlas Generation. *ACM Transactions on Graphics* 21, 3 (2002), 10–p.
- Lituan Harold Li, Pengchuan Zhang, Haotian Zhang, Jianwei Yang, Chunyuan Li, Yiwu Zhong, Lijuan Wang, Lu Yuan, Lei Zhang, Jenq-Neng Hwang, et al. 2022. Grounded language-image pre-training. In *Proceedings of the IEEE/CVF Conference on Computer Vision and Pattern Recognition*. 10965–10975.
- Cheng Lin, Tingxiang Fan, Wenping Wang, and Matthias Nießner. 2020a. Modeling 3d shapes by reinforcement learning. In *Computer Vision—ECCV 2020: 16th European Conference, Glasgow, UK, August 23–28, 2020, Proceedings, Part X 16*. Springer, 545–561.
- Cheng Lin, Changjian Li, Yuan Liu, Nenglu Chen, Yi-King Choi, and Wenping Wang. 2021. Point2skeleton: Learning skeletal representations from point clouds. In *Proceedings of the IEEE/CVF conference on computer vision and pattern recognition*. 4277–4286.
- Cheng Lin, Lingjie Liu, Changjian Li, Leif Kobbelt, Bin Wang, Shiqing Xin, and Wenping Wang. 2020b. Seg-mat: 3d shape segmentation using medial axis transform. *IEEE transactions on visualization and computer graphics* 28, 6 (2020), 2430–2444.
- Minghua Liu, Chao Xu, Haijin Jin, Linghao Chen, Zexiang Xu, Hao Su, et al. 2023c. One-2-3-45: Any single image to 3d mesh in 45 seconds without per-shape optimization. *arXiv preprint arXiv:2306.16928* (2023).
- Minghua Liu, Yinhao Zhu, Hong Cai, Shizhong Han, Zhan Ling, Fatih Porikli, and Hao Su. 2023d. Partslip: Low-shot part segmentation for 3d point clouds via pretrained image-language models. In *Proceedings of the IEEE/CVF Conference on Computer Vision and Pattern Recognition*. 21736–21746.
- Ruoshi Liu, Rundi Wu, Basile Van Hoorick, Pavel Tokmakov, Sergey Zakharov, and Carl Vondrick. 2023b. Zero-1-to-3: Zero-shot One Image to 3D Object. *CoRR abs/2303.11328* (2023).
- Weixiao Liu, Yuwei Wu, Sipu Ruan, and Gregory S Chirikjian. 2022. Robust and accurate superquadric recovery: A probabilistic approach. In *Proceedings of the IEEE/CVF Conference on Computer Vision and Pattern Recognition*. 2676–2685.
- Yuan Liu, Cheng Lin, Zijiao Zeng, Xiao Xiao Long, Lingjie Liu, Taku Komura, and Wenping Wang. 2023a. SyncDreamer: Generating Multiview-consistent Images from a Single-view Image. *arXiv preprint arXiv:2309.03453* (2023).
- Stuart Lloyd. 1982. Least squares quantization in PCM. *IEEE transactions on information theory* 28, 2 (1982), 129–137.
- Xiaoxiao Long, Yuan-Chen Guo, Cheng Lin, Yuan Liu, Zhiyang Dou, Lingjie Liu, Yuexin Ma, Song-Hai Zhang, Marc Habermann, Christian Theobalt, et al. 2023a. Wonder3D: Single Image to 3D using Cross-Domain Diffusion. *arXiv preprint arXiv:2310.15008* (2023).
- Xiaoxiao Long, Cheng Lin, Lingjie Liu, Yuan Liu, Peng Wang, Christian Theobalt, Taku Komura, and Wenping Wang. 2023b. Neuraludf: Learning unsigned distance fields for multi-view reconstruction of surfaces with arbitrary topologies. In *Proceedings of the IEEE/CVF Conference on Computer Vision and Pattern Recognition*. 20834–20843.
- Xiaoxiao Long, Cheng Lin, Peng Wang, Taku Komura, and Wenping Wang. 2022. Sparseneus: Fast generalizable neural surface reconstruction from sparse views. In *European Conference on Computer Vision*. Springer, 210–227.
- William E. Lorensen and Harvey E. Cline. 1987. Marching cubes: A high resolution 3D surface construction algorithm. In *Proceedings of the 14th Annual Conference on Computer Graphics and Interactive Techniques, SIGGRAPH 1987, Anaheim, California, USA, July 27-31, 1987*, Maureen C. Stone (Ed.). ACM, 163–169.
- Luke Melas-Kyriazi, Iro Laina, Christian Rupprecht, and Andrea Vedaldi. 2023. Realfusion: 360deg reconstruction of any object from a single image. In *Proceedings of the IEEE/CVF Conference on Computer Vision and Pattern Recognition*. 8446–8455.
- Ben Mildenhall, Pratul P Srinivasan, Matthew Tanck, Jonathan T Barron, Ravi Ramamoorthi, and Ren Ng. 2020. NeRF: Representing Scenes as Neural Radiance Fields for View Synthesis. In *European Conference on Computer Vision*. Springer, 405–421.
- Kaichun Mo, Paul Guerrero, Li Yi, Hao Su, Peter Wonka, Niloy J Mitra, and Leonidas J Guibas. 2019. StructureNet: hierarchical graph networks for 3D shape generation. *ACM Transactions on Graphics (TOG)* 38, 6 (2019), 1–19.
- George Kiyohiro Nakayama, Mikaela Angelina Uy, Jiahui Huang, Shi-Min Hu, Ke Li, and Leonidas Guibas. 2023. Diffacto: Controllable part-based 3d point cloud generation with cross diffusion. In *Proceedings of the IEEE/CVF International Conference on Computer Vision*. 14257–14267.
- Gimin Nam, Mariem Khelifi, Andrew Rodriguez, Alberto Tono, Linqi Zhou, and Paul Guerrero. 2022. 3d-ldm: Neural implicit 3d shape generation with latent diffusion models. *arXiv preprint arXiv:2212.00842* (2022).
- Alex Nichol, Heewoo Jun, Prafulla Dhariwal, Pamela Mishkin, and Mark Chen. 2022. Point-e: A system for generating 3d point clouds from complex prompts. *arXiv preprint arXiv:2212.08751* (2022).
- Chengjie Niu, Jun Li, and Kai Xu. 2018. Im2struct: Recovering 3d shape structure from a single rgb image. In *Proceedings of the IEEE conference on computer vision and pattern recognition*. 4521–4529.
- Aaron van den Oord, Yazhe Li, and Oriol Vinyals. 2018. Representation learning with contrastive predictive coding. *arXiv preprint arXiv:1807.03748* (2018).
- Despoina Paschalidou, Luc Van Gool, and Andreas Geiger. 2020. Learning unsupervised hierarchical part decomposition of 3d objects from a single rgb image. In *Proceedings of the IEEE/CVF Conference on Computer Vision and Pattern Recognition*. 1060–1070.
- Despoina Paschalidou, Angelos Katharopoulos, Andreas Geiger, and Sanja Fidler. 2021. Neural parts: Learning expressive 3d shape abstractions with invertible neural networks. In *Proceedings of the IEEE/CVF Conference on Computer Vision and Pattern Recognition*. 3204–3215.
- Despoina Paschalidou, Ali Osman Ulusoy, and Andreas Geiger. 2019. Superquadrics Revisited: Learning 3D Shape Parsing Beyond Cuboids. In *IEEE Conference on Computer Vision and Pattern Recognition, CVPR 2019, Long Beach, CA, USA, June 16-20, 2019*. Computer Vision Foundation / IEEE, 10344–10353.
- Dmitry Petrov, Mathieu Gadelha, Radomir Měch, and Evangelos Kalogerakis. 2023. ANISE: Assembly-based Neural Implicit Surface rEconstruction. *IEEE Transactions on Visualization and Computer Graphics* (2023).
- Ben Poole, Ajay Jain, Jonathan T Barron, and Ben Mildenhall. 2022. Dreamfusion: Text-to-3d using 2d diffusion. *arXiv preprint arXiv:2209.14988* (2022).
- Guocheng Qian, Jinjie Mai, Abdullah Hamdi, Jian Ren, Aliaksandr Siarohin, Bing Li, Hsin-Ying Lee, Ivan Skorokhodov, Peter Wonka, Sergey Tulyakov, et al. 2023. Magic123: One image to high-quality 3d object generation using both 2d and 3d diffusion priors. *arXiv preprint arXiv:2306.17843* (2023).
- Alec Radford, Jong Wook Kim, Chris Hallacy, Aditya Ramesh, Gabriel Goh, Sandhini Agarwal, Girish Sastry, Amanda Askell, Pamela Mishkin, Jack Clark, et al. 2021. Learning transferable visual models from natural language supervision. In *International conference on machine learning*. PMLR, 8748–8763.
- Amit Raj, Srinivas Kaza, Ben Poole, Michael Niemeyer, Nataniel Ruiz, Ben Mildenhall, Shiran Zada, Kfir Aberman, Michael Rubinstein, Jonathan Barron, et al. 2023. Dream-Booth3D: Subject-driven text-to-3d generation. *arXiv preprint arXiv:2303.13508* (2023).
- Rui SV Rodrigues, José FM Morgado, and Abel JP Gomes. 2018. Part-based mesh segmentation: a survey. In *Computer Graphics Forum*, Vol. 37. Wiley Online Library,

- 235–274.
- Pedro V Sander, Zoë J Wood, Steven Gortler, John Snyder, and Hugues Hoppe. 2003. Multi-chart geometry images. (2003).
- Lior Shapira, Ariel Shamir, and Daniel Cohen-Or. 2008. Consistent mesh partitioning and skeletonisation using the shape diameter function. *The Visual Computer* 24 (2008), 249–259.
- Shymon Shlafman, Ayellet Tal, and Sagi Katz. 2002. Metamorphosis of polyhedral surfaces using decomposition. In *Computer graphics forum*, Vol. 21. Wiley Online Library, 219–228.
- Zhenyu Shu, Chengwu Qi, Shi-Qing Xin, Chao Hu, Li Wang, Yu Zhang, and Ligang Liu. 2016. Unsupervised 3D shape segmentation and co-segmentation via deep learning. *Comput. Aided Geom. Des.* 43 (2016), 39–52.
- Jascha Sohl-Dickstein, Eric Weiss, Niru Maheswaranathan, and Surya Ganguli. 2015. Deep unsupervised learning using nonequilibrium thermodynamics. In *International conference on machine learning*. PMLR, 2256–2265.
- Robert W Sumner and Jovan Popović. 2004. Deformation transfer for triangle meshes. *ACM Transactions on graphics (TOG)* 23, 3 (2004), 399–405.
- Chun-Yu Sun and Qian-Fang Zou. 2019. Learning adaptive hierarchical cuboid abstractions of 3D shape collections. *ACM Trans. Graph.* 38, 6 (2019), 241:1–241:13.
- Stanislaw Szymanowicz, Christian Rupprecht, and Andrea Vedaldi. 2023. Viewset Diffusion:(0-) Image-Conditioned 3D Generative Models from 2D Data. *arXiv preprint arXiv:2306.07881* (2023).
- Ayça Takmaz, Elisabetta Fedele, Robert W Sumner, Marc Pollefeys, Federico Tombari, and Francis Engelmann. 2023. Openmask3d: Open-vocabulary 3d instance segmentation. *arXiv preprint arXiv:2306.13631* (2023).
- Junshu Tang, Tengfei Wang, Bo Zhang, Ting Zhang, Ran Yi, Lizhuang Ma, and Dong Chen. 2023. Make-it-3d: High-fidelity 3d creation from a single image with diffusion prior. *arXiv preprint arXiv:2303.14184* (2023).
- Guy Tevet, Sigal Raab, Brian Gordon, Yonatan Shafir, Daniel Cohen-Or, and Amit H Bermano. 2022. Human motion diffusion model. *arXiv preprint arXiv:2209.14916* (2022).
- Ayush Tewari, Tianwei Yin, George Cazenavette, Semon Rezhchikov, Joshua B Tenenbaum, Frédo Durand, William T Freeman, and Vincent Sitzmann. 2023. Diffusion with Forward Models: Solving Stochastic Inverse Problems Without Direct Supervision. *arXiv preprint arXiv:2306.11719* (2023).
- Shubham Tulsiani, Hao Su, Leonidas J. Guibas, Alexei A. Efros, and Jitendra Malik. 2017. Learning Shape Abstractions by Assembling Volumetric Primitives. In *2017 IEEE Conference on Computer Vision and Pattern Recognition, CVPR 2017, Honolulu, HI, USA, July 21–26, 2017*. IEEE Computer Society, 1466–1474.
- Arash Vahdat, Francis Williams, Zan Gojcic, Or Litany, Sanja Fidler, Karsten Kreis, et al. 2022. LION: Latent Point Diffusion Models for 3D Shape Generation. *Advances in Neural Information Processing Systems* 35 (2022), 10021–10039.
- Haochen Wang, Xiaodan Du, Jiahao Li, Raymond A Yeh, and Greg Shakhnarovich. 2023. Score jacobian chaining: Lifting pretrained 2d diffusion models for 3d generation. In *Proceedings of the IEEE/CVF Conference on Computer Vision and Pattern Recognition*. 12619–12629.
- Peng Wang, Lingjie Liu, Yuan Liu, Christian Theobalt, Taku Komura, and Wenping Wang. 2021. NeuS: Learning Neural Implicit Surfaces by Volume Rendering for Multi-view Reconstruction. *NeurIPS* (2021).
- Rundi Wu, Yixin Zhuang, Kai Xu, Hao Zhang, and Baoquan Chen. 2020. Pq-net: A generative part seq2seq network for 3d shapes. In *Proceedings of the IEEE/CVF Conference on Computer Vision and Pattern Recognition*. 829–838.
- Zhijie Wu, Xiang Wang, Di Lin, Dani Lischinski, Daniel Cohen-Or, and Hui Huang. 2019. Sagnet: Structure-aware generative network for 3d-shape modeling. *ACM Transactions on Graphics (TOG)* 38, 4 (2019), 1–14.
- Jianfeng Xiang, Jiaolong Yang, Binbin Huang, and Xin Tong. 2023. 3D-aware Image Generation using 2D Diffusion Models. *arXiv preprint arXiv:2303.17905* (2023).
- Desai Xie, Jiahao Li, Hao Tan, Xin Sun, Zhixin Shu, Yi Zhou, Sai Bi, Sören Pirk, and Arie E Kaufman. 2023. Carve3D: Improving Multi-view Reconstruction Consistency for Diffusion Models with RL Finetuning. *arXiv preprint arXiv:2312.13980* (2023).
- Dejia Xu, Yifan Jiang, Peihao Wang, Zhiwen Fan, Yi Wang, and Zhangyang Wang. 2023. NeuralLift-360: Lifting an In-the-Wild 2D Photo to a 3D Object With 360deg Views. In *Proceedings of the IEEE/CVF Conference on Computer Vision and Pattern Recognition*. 4479–4489.
- Hao Tian Xu, Ming Dong, and Zichun Zhong. 2017. Directionally Convolutional Networks for 3D Shape Segmentation. In *IEEE International Conference on Computer Vision, ICCV 2017, Venice, Italy, October 22–29, 2017*. IEEE Computer Society, 2717–2726.
- Yunhan Yang, Xiaoyang Wu, Tong He, Hengshuang Zhao, and Xihui Liu. 2023. SAM3D: Segment Anything in 3D Scenes. *arXiv preprint arXiv:2306.03908* (2023).
- Qing Yuan, Guiqing Li, Kai Xu, Xudong Chen, and Hui Huang. 2016. Space-time co-segmentation of articulated point cloud sequences. In *Computer Graphics Forum*, Vol. 35. Wiley Online Library, 419–429.
- Wangyu Zhang, Bailin Deng, Juyong Zhang, Sofien Bouaziz, and Ligang Liu. 2015. Guided Mesh Normal Filtering. *Comput. Graph. Forum* 34, 7 (2015), 23–34.
- Xin-Yang Zheng, Hao Pan, Peng-Shuai Wang, Xin Tong, Yang Liu, and Heung-Yeung Shum. 2023. Locally attentional sdf diffusion for controllable 3d shape generation. *arXiv preprint arXiv:2305.04461* (2023).
- Youyi Zheng, Hongbo Fu, Oscar Kin-Chung Au, and Chiew-Lan Tai. 2011. Bilateral Normal Filtering for Mesh Denoising. *IEEE Trans. Vis. Comput. Graph.* 17, 10 (2011), 1521–1530.
- Yan Zheng, Lemeng Wu, Xingchao Liu, Zhen Chen, Qiang Liu, and Qixing Huang. 2022. Neural volumetric mesh generator. *arXiv preprint arXiv:2210.03158* (2022).
- Wenyang Zhou, Zhiyang Dou, Zeyu Cao, Zhouyingcheng Liao, Jingbo Wang, Wenjia Wang, Yuan Liu, Taku Komura, Wenping Wang, and Lingjie Liu. 2023. EMDM: Efficient Motion Diffusion Model for Fast, High-Quality Motion Generation. *arXiv preprint arXiv:2312.02256* (2023).
- Emanoil Zuckerman, Ayellet Tal, and Shymon Shlafman. 2002. Polyhedral surface decomposition with applications. *Computers & Graphics* 26, 5 (2002), 733–743.